Journal of Engineering and Technology for Industrial Applications

ITEGAM-JETIA

Manaus, v.10 n.49, p. 1-11. September/October., 2024.
DOI: https://doi.org/10.5935/jetia.v10i49.996

ISSN ONLINE: 2447-0228

RESEARCH ARTICLE OPEN ACCESS

CONVOLUTIONAL NEURAL NETWORKS AND DEEP LEARNING FOR THE DETECTION OF PNEUMONIA IN X-RAY IMAGES

Robinson Joel M[1], Ebenezer V[2], Manikandan G[3], Gokulaselvam R[4], Bharath R K[5] and Praveen Kumar R[6],

[1]Associate Professor, Department of Computer Science and Engineering, KCG College of Technology,Chennai, India.
[2]Assistant Professor, Division of Data Science and Cyber Security, Karunya Institute of Technology and Sciences, Coimbatore, India
[3]Professor, Department of Artificial intelligence and Data Science, R.M.K. Engineering College, Tiruvallur, India.
[4,5,6]Department of Information Technology, Kings Engineering College, Chennai.

[1]http://orcid.org/0000-0002-3030-8431, [2]http://orcid.org/0000-0002-0801-6926, [3]http://orcid.org/0000-0002-4323-8233
[4]http://orcid.org/0009-0000-6502-022X, [5]http://orcid.org0009-0002-7456-4506, [6]http://orcid.org0009-0007-3903-9438,

Email: [1]joelnazareth@gmail.com, [2]ebenezerv@karunya.edu, [3]mani4876@gmail.com, [4]gokulaselvamravindran@gmail.com, [5]bharnish888@gmail.com, [6]praveenkumarrethinam@gmail.com

ARTICLE INFO

Article History
Received: December 13th, 2023
Revised: September 06th, 2024
Accepted: September 06th, 2024
Published: Month 30th, 2024

Keywords:
X-Ray,
Artificial Intelligence,
Radiologist,
Data accessibility,
Accuracy.

ABSTRACT

Artificial intelligence has been used in a variety of industries during the course of its growth, especially over the past decade as a result of the enormous rise in data accessibility. Its main objective is to assist people in making judgements that are more reliable, quick, and accurate. The usage of machine learning and artificial intelligence in the medical profession is growing. This is especially true for medical fields that employ a variety of biological picture kinds and where diagnostic procedures rely on collecting and analysing a substantial amount of digital data. Machine learning-based evaluation of medical photos enhances reporting uniformity and accuracy. In order to help decision-makers make the most accurate diagnosis, this study promotes the use of machine learning algorithms to evaluate chest X-ray images. With the aid of the CNN (Convolutional Neural Network) algorithm, the process will "learn" based on previously collected X-ray data from both healthy and sick patients (the training set). This research provides an approach to photo interpretation based on deep learning. This technique will reduce radiologists' burden because of its accuracy of more than 91% and nearly immediate findings, especially for those who must analyse an extensive amount of patient pictures.

Copyright ©2024 by authors and Galileo Institute of Technology and Education of the Amazon (ITEGAM). This work is licensed under the Creative Commons Attribution International License (CC BY 4.0).

I INTRODUCTION

Pneumonia is an inflammatory disease that affects the air sacs in either or both of the lungs. It can be brought on by a variety of infectious agents, including organisms such as bacteria, viruses, fungi, as well as certain chemicals. Pneumonia can range in severity from mild to severe, and it can have negative effects, especially in vulnerable populations including young children of all ages, the elderly, and people with weakened immune systems. Typically, a combination of physical exams, chest X-rays, lab testing, and perhaps sputum cultures are used to diagnose pneumonia.

Even though artificial intelligence (AI) [1] was acknowledged as a field of study at the start of the twentieth century, scientific communities did not look into it in depth for a very long time due to its poor applicability. Due to the rise of processing power and the accumulation of enormous amounts of data over the past 20 years, AI has attracted interest from the educational and industry sectors. Throughout the several "Seasons of AI" that AI underwent during its development, there were various stages. The period spanning from the start of the 20th century to the present, which is sometimes described as the "AI Winter," used to be the most well known season of AI. This fact is one of the main reasons why AI at this point could not develop fast.

Pneumonia [2], a viral lung disease, primarily affects the pulmonary capillaries and prevents oxygen from entering the bloodstream. Coughing, pain in the chest, a high body temperature, and breathing difficulties are typical symptoms. Most typically, pneumonia is brought on by bacterial, viral, or autoimmune conditions. Blood tests and chest X-rays are used to identify inflammation. The corona virus (Covid-19) [3], whose patients are at a higher risk of developing pneumonia, is relevant in terms of

test accuracy and decoding speed at this time. The current significant increase in patients need a rapid and accurate solution for interpreting the X-rays. A Deep Learning-based technique for picture decoding is demonstrated in this paper. Since it yields findings almost immediately and with a precision level of over 90%, this technology will be used to reduce the burden of radiologists whom must evaluate a huge number of patient images. With the aid of the CNN (Convolutional Neural Network) algorithm [4], the process will "learn" based on previously collected X-ray data from both healthy and sick patients (the training set).

To tackle the issue, you must create a deep network. The initial objective of the network's depth is the chance that the picture reflects a confirmed case of pneumonia. The range of the likelihood ranges from 0 to 1, with 1 denoting a specific instance of pneumonia. The test picture set, which is entirely different from the training set, will be used to assess performance. A probability of error of no more than ten percent, or an accuracy rate of more than 90%, will be regarded as good achievement.

Construct the PRECISION and the RECALL [5] effectiveness graph for the network you choose, with each point on the graph generated for an alternative threshold level) in proportion to the likelihood the network produced (to choose a positive example, such as pneumonia. The threshold for each value will be in increments of 05.0 from 1.0 to 9.0. Mark the SCORE-F scores [5] that are going to be determined based on each pair of PRECISION-RECALL numbers on the diagram as well. What criteria yielded the greatest SCORE-F value? Try some of the following modifications to increase accuracy and effectiveness for the internet connection you chose: Introduction of one layer as per your option; the decision must be supported. Incorporation of two additional layers as per your option; the choice that you make must be supported.

Examine five modifications to the total amount of kernels used for convolution (no extra layers) and/or the depth of the current layers. The decision must be supported. Use the following training methods to assess the network's performance. Examine how the EPOCHS [6] and APPROACHING number RATEs affect the algorithm: SGD algorithm, including both MOMENTUM and MOMENTUM, as options NESTEROV [7]. Algorithm ADAM [8], RMSPROP algorithm [9]. Analyse the impact of the following modifications with dropout in the event there is a layer, see what happens if its likelihood DROPOUT's [10] parameter is changed.

II RELATED WORK

Radiographs [11], usually referred to as X-ray pictures, are an important diagnostic tool in the medical industry and several other industries. They are made by exposing a body or an item to X-rays and then recording the radiation that results on a specialised detector or film. An electromagnetic radiation with a greater energy than visible light is an x-ray. When X-rays travel through an item, solid tissues like bones absorb them while less dense tissues like muscles and organs disperse them. An image that resembles a shadow is produced when a detector on the opposite side of the item records the fluctuating X-ray exposure levels.

The initial step before building a model is often preprocessing the input data. The images were uploaded as grayscale for the purpose of the study after being scaled down from their original RGB colour space to 200x200 pixels. The pixel intensity levels were then normalised by dividing the pixel values by 255. In this way, the pixels in the image are represented by floating point integers between 0 and 1, rather than utilising integer numbers from 0 to 255. This should positively affect CNN's performance.

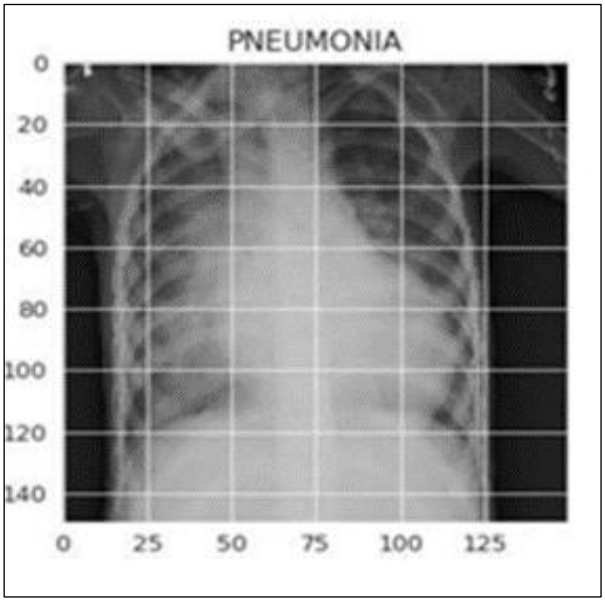

Figure 1: A chest X-ray labeled as pneumonia.
Source: Authors, (2024).

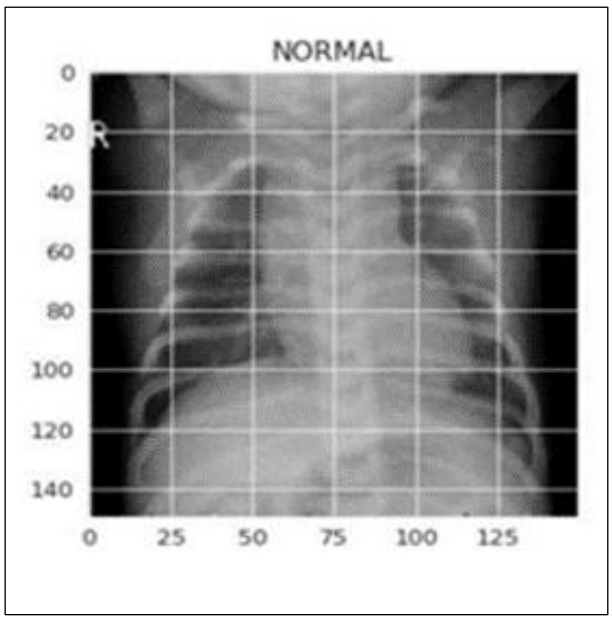

Figure 2: A chest X-ray labeled as normal.
Source: Authors, (2024).

An artificial neural network called a convolutional neural network (CNN or ConvNet) is specialised for processing and analysing visual input, such as pictures and movies. Many computer vision applications, such as image classification, object identification, picture segmentation, and others, have seen significant success with CNNs. They are especially successful at tasks requiring sequential feature extraction because they are modelled after the structure and operation of the visual system in humans.

The foundational units of CNNs are convolutional layers. They compute the number of dots at each place by scanning over the input picture with convolutional filters, commonly called as kernels. The network can recognise characteristics like borders, materials, and patterns thanks to this action. Activation functions, such as ReLU, are frequently added after convolutional layers to add non-linearity. The geographic dimensions of the map of features created by convolutional layers are decreased by pooling layers, also known as subsampling or down-sampling layers. By doing so, computation is reduced and the network is strengthened

against changes in input. Max-pooling and average-pooling are two common pooling techniques.

The applications like Numpy, one of the python lass Pandas, the another class is Keras, the platform is Jupyter Notebook, to map the chart matplotlib used, and seaborn were extensively utilised in this example. The model was trained and evaluated locally using a PC equipped with an processor AMD Ryzen 5 with the speed of 3600 CPU, and RAM memory space of 16GB of 3200MHz speed RAM. The model has to be trained for up to 90 minutes. The photos were categorised using a machine learning technique based on CNN. The CNN is an instance of deep learning neural networks. The most popular applications for CNNs in picture classification and identification mark a substantial development in these domains. Input and output are just a couple of the layers that make them up, with hidden layers placed in between.

Convolutional neural networks (CNNs) and deep learning are two fields where the term "Conv2D" is frequently used. It speaks about a particular kind of layer that neural networks employ to interpret two-dimensional input, such as photographs. A neural network's Conv2D layer convolutionally processes the input data using a series of adaptive filters or kernels. These filters "convolve" or glide across the information that is entered to create feature maps that draw attention to key patterns or characteristics. A Conv2D layer produces a collection of feature maps, which are then utilised as inputs by different layers in the network's architecture.

Rectified Linear Unit, or ReLU, is a popular function of activation in artificial neural networks, particularly deep learning models. It is used to add non-linearity to the model by applying it to the final result of a single neuron or a layer of a neural network. The following is a definition of the ReLU activation function, which is max (0, x) = f(x). In the above formula, "x" stands for the function's input and "f(x)" for the output. The ReLU procedure is straightforward yet efficient. The value "x" is returned in its original form if the input is affirmative (f(x) = x). It returns zero if the input value "x" is negative or 0 (f(x) = 0).

ReLU is highly computational since it just uses the max function and simple mathematical operations; it doesn't need exponential functions or other sophisticated calculations. ReLU enables neural networks to describe complicated, nonlinear connections in data by introducing nonlinearity into the network. For deep learning models to be successful, this is essential. The network may become sparse as a result of ReLU. Only a portion of neurons are active at any given moment since negative values are assigned to zero, which might help with capacity for modelling and training efficiency.

Convolutional neural networks (CNNs) frequently employ the MaxPool2D layer for the processing of images and other 2D input. It is mostly employed to down-sample or subsample an input tensor, so lowering its geographic dimensions while preserving crucial data. Max pooling is a type of layer of pooling that chooses the highest value from a collection of values inside a predetermined area of the tensor that was input.

Flattening as shown in the figure is a frequently used procedure in a variety of programming tasks, particularly when working with layered data, tree structures, or processing information. You may streamline data structures and have easier access to elements for analysis or change. A crucial stage in CNN, we shall employ it when flat output is desired. The Classifier layer, which sits above the classification layer, is where we will attempt to convert a matrix with two dimensions towards vector values.

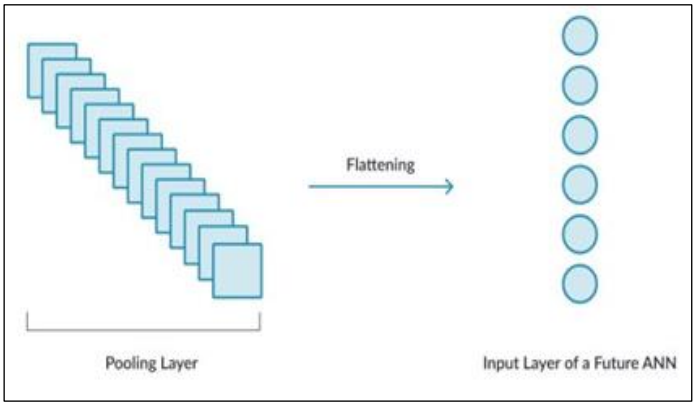

Figure 3: Layer Architecture.
Source: Authors, (2024).

A layer as shown in the figure is said to be dense if each of the neurons in the topmost layer obtains input from every neuron in the layer below it. The most prevalent layer in models was shown to be the thick layer. The layer multiplies a product by a matrix in the background, having the matrix contents acting as verifiable weights. The layer's function is to really modify the vector dimension because the layer's origin is a vector.

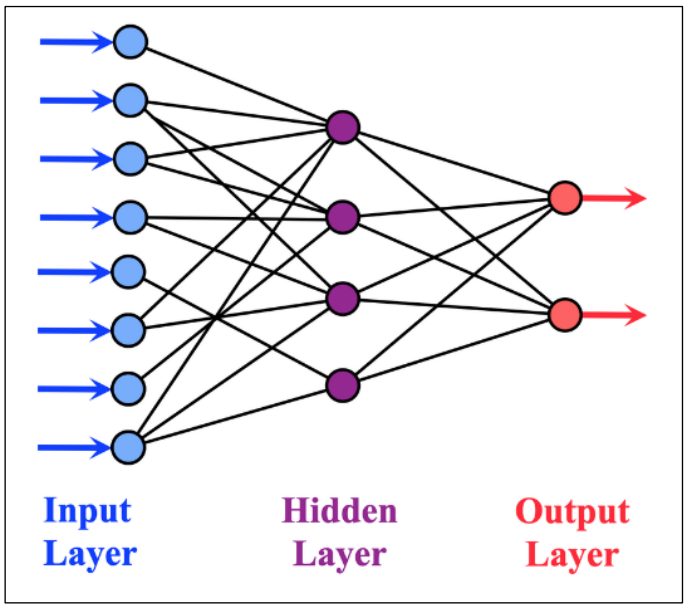

Figure 4: A shallow neural network with a Dense layer.
Source: Authors, (2024).

Sets the number of pictures in the control set, for example, as well as the size of the representative group used for training. The number of epochs (which partition the collection into groupings according to the number of epochs when compared to various sample groups) that we train using a particular sample group. Loss Function: A loss function is a mathematical formula that converts the values of any number of parameters into a precise figure that reflects the "cost" of a certain occurrence. This feature is used to do optimisation with the goal of minimising output.

III RESULTS AND DISCUSSION

In this study, 5,863 genuine X-rays of pneumonia victims as well as healthy individuals were found in an archive downloaded from the Kaggle website. Three folders are used to organise the photographs in the database. During the learning process, the set of training images is a collection of samples (labelled pictures) that is used to alter parameters, such as weights. Validation - The

validation set, a different set used for control throughout the training process, allows for increasing the hyperparameters (such as training rate) that are often not changed during training, hence enhancing the categorization level of the pictures. There are 8 photographs in the series without pneumonia and 8 images with pneumonia.

The set of test images is a collection of untagged pictures used to evaluate the performance of the network by putting it to the test after training. In summary, the operating principle is: The system is first trained (Train). The system is currently learning how to recognise photos using a variety of criteria and weights. The testing step comes next. We are now checking each image individually without tags. Finally, we contrast the verification control set, which truly evaluates the degree of learning success in the learnt parameters. Through here, we arrive at a specific accuracy, expressed in percent (Accuracy).

The Recall-Precision graph, whose points are produced for various threshold levels in proportion to the likelihood the network generates for selecting a personal example, describes the performance of the fundamental model. Table 1 shows that the greatest average harmonic (F1 -Score) is 0.8556825 and that it happens for a threshold for probability level of 0.4, meaning that the best performance will be obtained if designate that all samples where the likelihood is beneficial (positive for pneumonia) will be beyond 0.4 as shown in Figure 5.

Table 1: Description of the performance of the Recall-Precision.

Threshold	Recall	Precision	F-Score:
0.1	0.9688	0.65207	0.7794947
0.15	0.9585	0.69556	0.8061705
0.2	0.9449	0.73047	0.8240016
0.25	0.9303	0.76085	0.8370907
0.3	0.9150	0.78751	0.8465588
0.35	0.8995	0.81027	0.8525626
0.4	0.8844	0.82872	0.8556825
0.45	0.8650	0.8453	0.8550874
0.5	0.8471	0.86024	0.8536374
0.55	0.8250	0.88944	0.8498365
0.6	0.8007	0.90215	0.842791
0.65	0.7735	0.91522	0.8329102
0.7	0.74410	0.92686	0.8208399
0.75	0.70428	0.92683	0.8003814
0.8	0.65540	0.9368	0.7712586
0.85	0.5896971	0.9494	0.7275372
0.9	0.4970978	0.9642	0.7560144

Source: Authors, (2024).

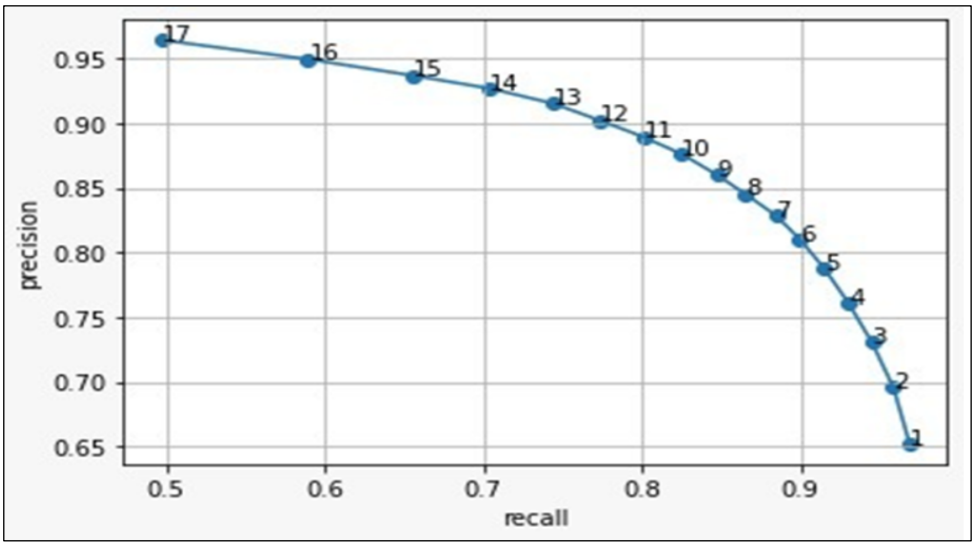

Figure 5: Recall-Precision graph.
Source: Authors, (2024).

Table 2: Result for the different kernel, for Conf2D, and for Max pool.

Methods followed as	Loss of the model	Accuracy
depth of convolution = 32	0.27854	0.9087
depth of convolution =64	0.269219	0.879
depth of convolution =128	0.4191	0.8349
addition of two 32 layers	0.2069	0.9199
addition of two 64 layers	0.268848	0.9006
one layer of 32 and one of 64	0.369782	0.8638
one layer of 64 and 128 Layer	0.30123	0.891
reducing the kernels of the convolution to (2X2)	0.2755	0.891
reducing the kernels of the convolution to (4X4)	0.2527	0.9119
Reducing dense layer to 32	0.28824	0.9103
Layers depth are doubled	0.28439	0.9151
Increasing kernels on each layer	0.48511	0.8349

Source: Authors, (2024).

Table 3: Result for the different kernel, for Conf2D, and for Max pool.

Methods followed as	recall	precision	Accuracy in %
depth of convolution = 32	0.82	0.8245	90.87%
depth of convolution =64	0.8295	0.834	87.98%
depth of convolution =128	0.807	0.8155	83.49%
addition of two 32 layers	0.7991	0.809	91.99%
addition of two 64 layers	0.8014	0.8103	90.06%
one layer of 32 and one of 64	0.8042	0.8135	86.38%
one layer of 64 and 128 Layer	0.8065	0.8157	89.10%
reducing the kernels of the convolution to (2X2)	0.7731	0.7936	89.10%
reducing the kernels of the convolution to (4X4)	0.7889	0.8016	91.19%
Reducing dense layer to 32	0.813	0.8261	91.03%
Layers depth are doubled	0.7903	0.8094	91.51%
Increasing kernels on each layer	0.777	0.7963	83.499

Source: Authors, (2024).

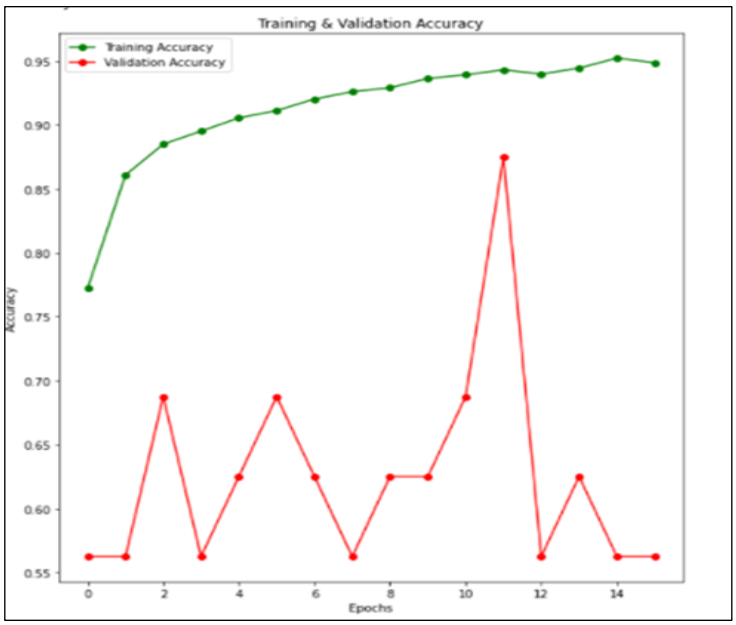

Figure 6a: Training and Testing validation accuracy and its loss against epochs.
Source: Authors, (2024).

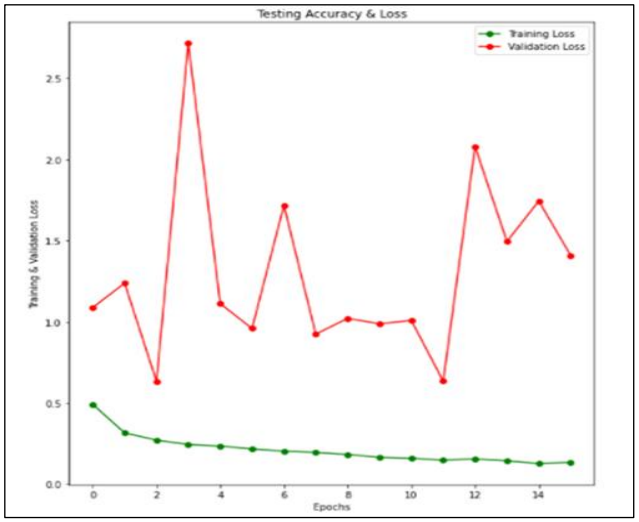

Figure 6b: Training and Testing validation accuracy and its loss against epochs.
Source: Authors, (2024).

The above figure 6a and Figure 6b also table 2 and table 3 shows the accuracy chart that there is a decline in the 12th repetition and a regularity beginning with the 10th iteration. It is evident from the decrease in the graph that some oscillations cause the learning rate lowering mechanism to become active. In any event, the system's accuracy stays at about 90%. Lets employ this strategy after coming to the ultimate judgement that extending the convolution to depth 32 produced the highest accuracy enhancement of 90.8%.

Table 4: Stochastic Gradient Descent with Different Learning Rates and Epochs.

SGD	Loss of the model	accuracy
SGD learning rate=0.05, Epochs num=8	0.4024	0.8574
SGD Learning rate=0.001 Epochs=16	0.7018	0.625
SGD Learning rate=0.0001 Epochs =32	0.6805	0.625
SGD+Momentum=0.4 +Nesterov=True	0.4117	0.8766
learning rate=0.0001 epochs=16	0.6697	0.625
SGD+Momentum=0.8 +Nesterov=True		
learning rate = 0.05 epochs=8	0.4052	0.7965
learning rate = 0.05 epochs= 16	0.6961	0.625

Source: Authors, (2024).

Table5: Stochastic Gradient Descent with Different Learning Rates and Epochs.

SGD	recall	precision	Accuracy in %
SGD learning rate=0.05, Epochs num=8	0.5814	0.7194	85.74%
SGD Learning rate=0.001 Epochs=16	0.2579	0.1436	62.50%
SGD Learning rate=0.0001 Epochs =32	0.5006	0.1452	62.50%
SGD+Momentum=0.4 +Nesterov=True	0.6306	0.7383	87.66%
learning rate=0.0001 epochs=16	0.4505	0.1474	62.50%
SGD+Momentum=0.8 +Nesterov=True			
learning rate = 0.05 epochs=8	0.5356	0.6973	79.65%
learning rate = 0.05 epochs= 16	0.268	0.1466	62.50%

Source: Authors, (2024).

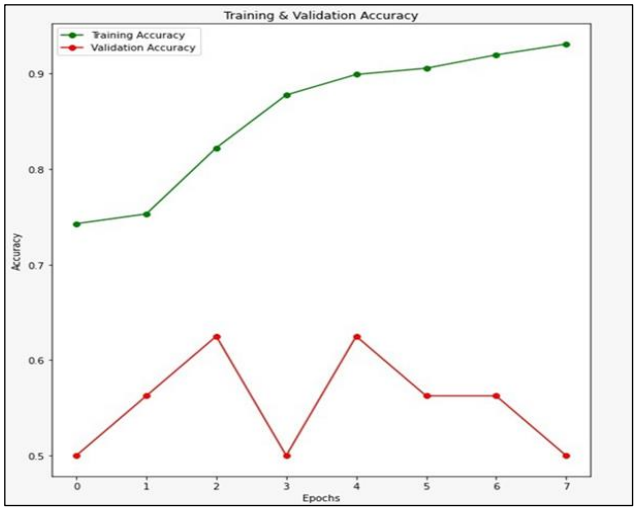

Figure 7a: Training and Testing validation accuracy and its loss against epochs.
Source: Authors, (2024).

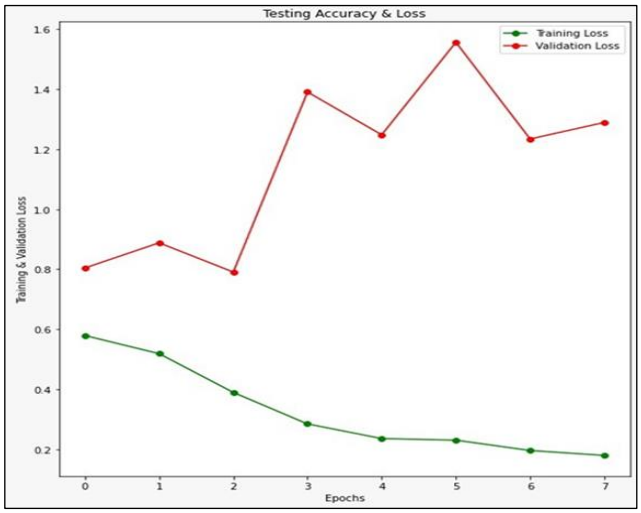

Figure 7b: Training and Testing validation accuracy and its loss against epochs.
Source: Authors, (2024).

s shown in the Figure 7a and Figure 7b also Table 4 and Table 5, the optimizer (SGD) clearly produces results below the 90% accuracy threshold, we will not be using it. We will not be using this optimizer given that it is clear that we were not able to achieve the 90% accuracy level with Nesterov and this strategy (SGD + Momentum).

When deep neural networks with several layers are being trained or when various model parameters have varying scales, Root Mean Squared Propagation noted as RMSProp is very helpful. When compared to approaches that use fixed learning rates, such stochastic gradient descent (SGD), it facilitates the individual adaptation of learning processes for each parameters vary resulting in more rapid convergence and greater performance.

Table 6: Root Mean Squared Propagation with different Learning Rate and different epochs.

RMSProp	Loss of the model	accuracy
learning rate=0.0001 epochs =8	0.6955	0.625
learning rate=0.0001 epochs =16	0.5228	0.8317
learning rate=0.001 epochs=16	0.3556	0.9054
learning rate=0.001 epochs=8	0.3095	0.891
learning rate=0.001 epochs=32	0.3874	0.9006

Source: Authors, (2024).

Table 7: Root Mean Squared Propagation with different Learning Rate and different epochs.

RMSProp	recall	precision	Accuracy in %
learning rate=0.0001 epochs =8	0.2272	0.2684	62.50%
learning rate=0.0001 epochs =16	0.6938	0.7694	83.17%
learning rate=0.001 epochs=16	0.8099	0.8389	90.54%
learning rate=0.001 epochs=8	0.7277	0.7822	89.10%
learning rate=0.001 epochs=32	0.8508	0.871	90.06%

Source: Authors, (2024).

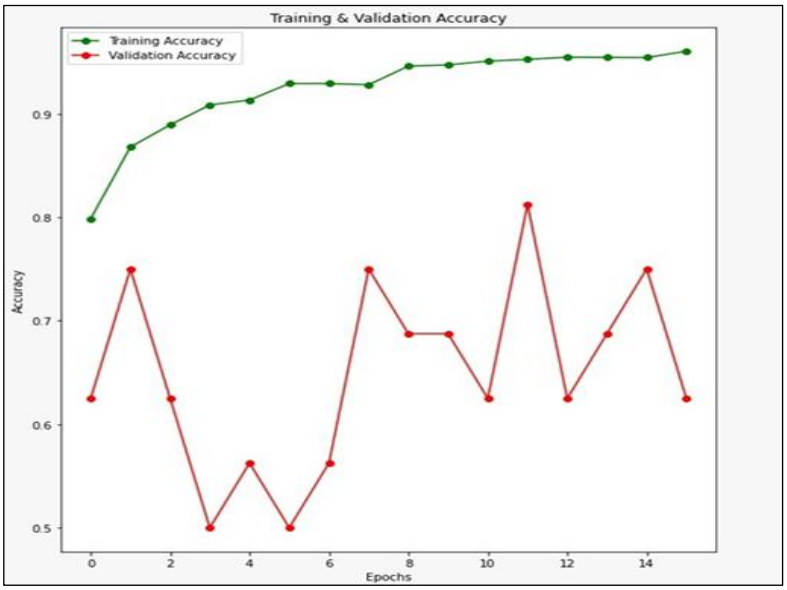

Figure 8a: Training and Testing validation accuracy and its loss against epochs
Source: Authors, (2024).

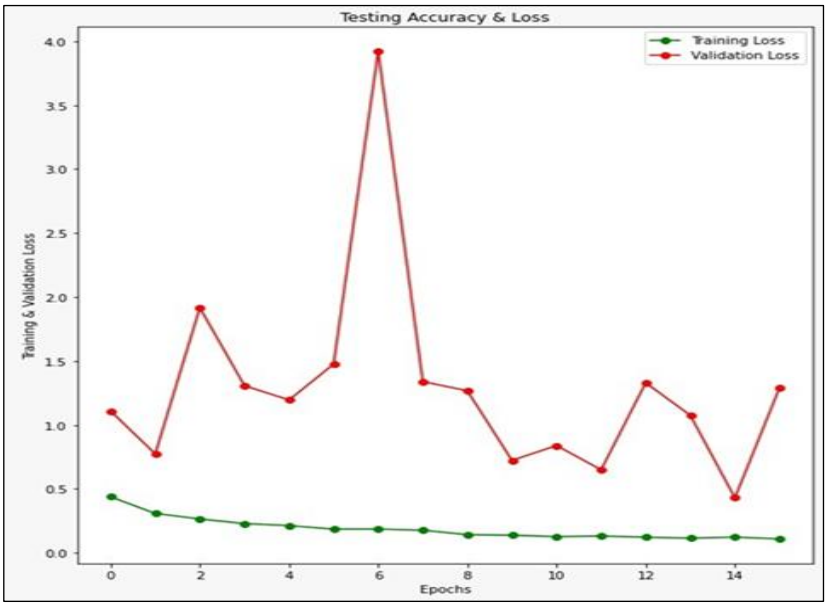

Figure 8b: Training and Testing validation accuracy and its loss against epochs
Source: Authors, (2024).

As shown in the Table 6 and Table 7 also Figure 8a and Figure 8b, different learning rates and different epochs are applied on the dataset. In machine learning and optimisation, "Root Mean Squared Propagation" does not constitute an often used word or algorithm. You could have meant "Root Mean Square Propagation," which might have been a potential misspelling or variant of the widely used optimisation process known as "RMSprop." As shown in the Figure 9 and Figure 10, the Recall and Precision with different Learning Rates and different epochs are measured and accuracy of the model also measured.

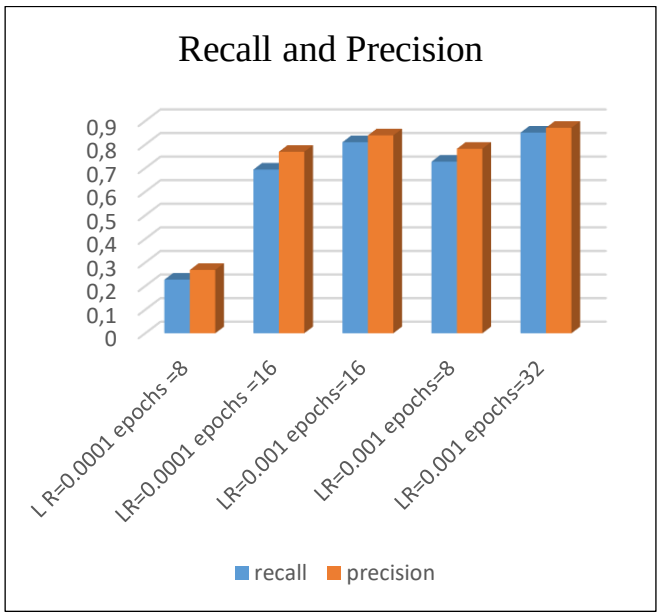

Figure9: RMSP Recall and Precision with different Learning Rates and different epochs.
Source: Authors, (2024).

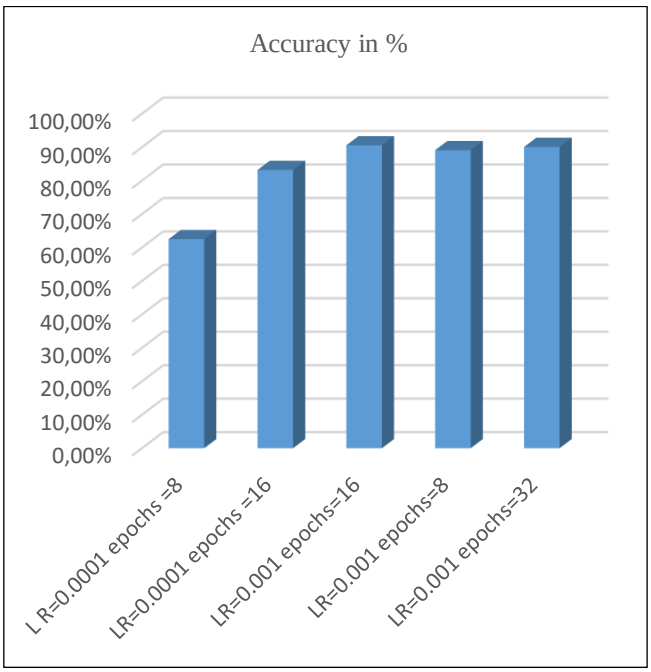

Figure 10: RMSP Accuracy with different Learning Rates and different epochs.
Source: Authors, (2024).

The chance of training a specific node in a layer is the default meaning of the dropout hyperparameter, where 1.0 denotes no dropout and 0.0 denotes no outputs from the layer. Around 0.5 and 0.8 is an acceptable range for dropout within a layer that is hidden. The dropout rate for input layers is higher, typically 0.8. From the equation 1 and 2 we can find out the dropout algorithm.

$$z_i^{(l+1)} = w_i^{(l+1)} y^l + b_i^{(l+1)} \quad \text{------(1)}$$

$$y_i^{(l+1)} = f(z_i^{(l+1)}) \quad \text{------(2)}$$

Table 8: Value generated for different dropout rate.

Dropout	Loss of the model	accuracy
dropout=0.1	0.2978	0.9038
dropout=0.2	0.3578	0.9022
Dropout =0.3	0.3332	0.8942
Dropout =0.4	0.3126	0.9135

Source: Authors, (2024).

Table 9: Value generated for different dropout rate.

Dropout	recall	precision	Accuracy in %
dropout=0.1	0.77	0.8215	90.38%
dropout=0.2	0.786	0.832	90.22%
Dropout =0.3	0.7776	0.8315	89.42%
Dropout =0.4	0.7416	0.8137	91.35%

Source: Authors, (2024).

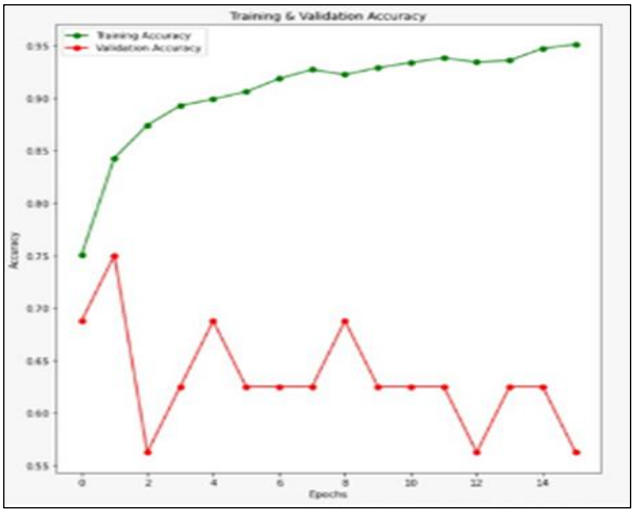

Figure 11a: Training and Testing validation accuracy and its loss against epochs.
Source: Authors, (2024).

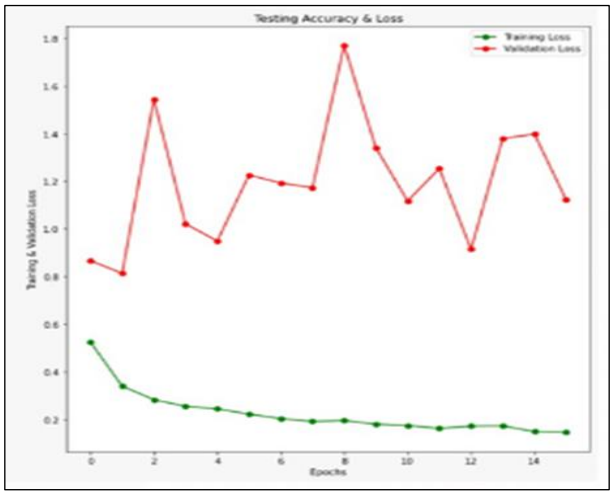

Figure 11b: Training and Testing validation accuracy and its loss against epochs.
Source: Authors, (2024).

Figure 8a & Figure 8b, Figure 9a & Figure 9b, Figure 10a & Figure 10b, and Figure 11a & Figure 11b shows the Training and Testing validation accuracy and its loss against epochs. Dropout is a regularisation approach in machine learning as shown in Table 8 and Table 9 that keeps neural networks from overfitting. When a machine learning algorithm learns the set used for training too thoroughly—including the noise and outliers—it is said to be overfitting, and this results in poor generalisation on fresh, untried data. A method called "dropout" is intended to deal with this problem. It involves randomly "dropping out" (that is, setting to zero) a certain percentage of the components (neurons) in an artificial neural network during development. During every training iteration, a randomised fraction of neurons is selected to be deactivated or "dropped out". These neurons that have fallen out have zero output. This altered data is used to train the neural network.

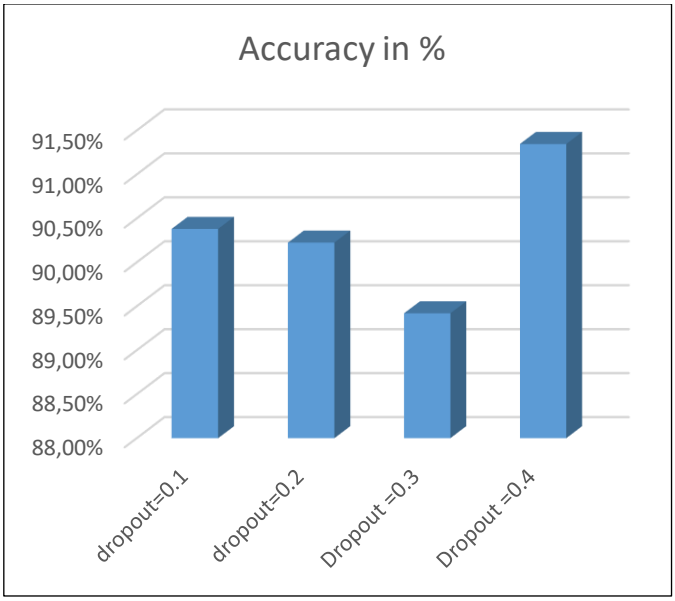

Figure 12: Accuracy with different Learning Rates and different epochs using Dropout.
Source: Authors, (2024).

Accuracy with different Learning Rates and different epochs suing dropout is shown in figure 12.

IV. CONCLUSION

Throughout the development of artificial intelligence, many different businesses have employed it, particularly in the last ten years due to the tremendous increase in data accessibility. Its fundamental goal is to help individuals make decisions that are more trustworthy, rapid, and accurate. Artificial intelligence and machine learning are increasingly being used in the medical field. This is particularly relevant for medical professions where diagnostic processes depend on gathering and interpreting substantial amounts of digital data and which use a range of biological image types. The examination of medical images using machine learning improves the accuracy and consistency of reporting. This study encourages the application of machine learning algorithms to assess chest X-ray pictures in order to aid decision-makers in making the most precise diagnosis. The procedure will "learn" based on previously athered X-ray information on both normal and sick patients (the training set), using the CNN (Convolutional Neural Network) algorithm. Thus work offers a deep learning-based method for interpreting photos. Because of this technique's over 91% accuracy and almost instantaneous results, radiologists will have less work to do—especially those who have to analyse a large number of patient images.

V. REFERENCES

[1] H. WANG, Y. LIU, Z. HAN and J. WU, "Extension of media literacy from the perspective of artificial intelligence and implementation strategies of artificial intelligence courses in junior high schools," *2020 International Conference on Artificial Intelligence and Education (ICAIE)*, Tianjin, China, 2020, pp. 63-66, doi: 10.1109/ICAIE50891.2020.00022.

[2] A. Serener and S. Serte, "Deep learning for mycoplasma pneumonia discrimination from pneumonias like COVID-19," 2020 4th International Symposium on Multidisciplinary Studies and Innovative Technologies (ISMSIT), Istanbul, Turkey, 2020, pp. 1-5, doi: 10.1109/ISMSIT50672.2020.9254561.

[3] S. Kurahashi, "Estimating Effectiveness of Preventing Measures for 2019 Novel Coronavirus Diseases (COVID-19)," 2020 9th International Congress on Advanced Applied Informatics (IIAI-AAI), Kitakyushu, Japan, 2020, pp. 487-492, doi: 10.1109/IIAI-AAI50415.2020.00103.

[4] R. Xin, J. Zhang and Y. Shao, "Complex network classification with convolutional neural network," in Tsinghua Science and Technology, vol. 25, no. 4, pp. 447-457, Aug. 2020, doi: 10.26599/TST.2019.9010055.

[5] S. A. Khan and Z. Ali Rana, "Evaluating Performance of Software Defect Prediction Models Using Area Under Precision-Recall Curve (AUC-PR)," 2019 2nd International Conference on Advancements in Computational Sciences (ICACS), Lahore, Pakistan, 2019, pp. 1-6, doi: 10.23919/ICACS.2019.8689135.

[6] N. Adiga, D. Govind and S. R. Mahadeva Prasanna, "Significance of epoch identification accuracy for prosody modification," 2014 International Conference on Signal Processing and Communications (SPCOM), Bangalore, India, 2014, pp. 1-6, doi: 10.1109/SPCOM.2014.6984007.

[7] P. Gu, S. Tian and Y. Chen, "Iterative Learning Control Based on Nesterov Accelerated Gradient Method," in IEEE Access, vol. 7, pp. 115836-115842, 2019, doi: 10.1109/ACCESS.2019.2936044.

[8] S. Peng, W. Li, D. Guo and H. Peng, "Efficiency optimization control of interior permanent magnet synchronous motor based on Adam algorithm," 2023 International Symposium on Signals, Circuits and Systems (ISSCS), Iasi, Romania, 2023, pp. 1-4, doi: 10.1109/ISSCS58449.2023.10190871.

[9] M. A. Labbaf Khaniki, M. Behzad Hadi and M. Manthouri, "Feedback Error Learning Controller based on RMSprop and Salp Swarm Algorithm for Automatic Voltage Regulator System," 2020 10th International Conference on Computer and Knowledge Engineering (ICCKE), Mashhad, Iran, 2020, pp. 425-430, doi: 10.1109/ICCKE50421.2020.9303718.

[10] N. Bacanin, E. Tuba, T. Bezdan, I. Strumberger, R. Jovanovic and M. Tuba, "Dropout Probability Estimation in Convolutional Neural Networks by the Enhanced Bat Algorithm," 2020 International Joint Conference on Neural Networks (IJCNN), Glasgow, UK, 2020, pp. 1-7, doi: 10.1109/IJCNN48605.2020.9206864.

[11] O. Nomir and M. Abdel-Mottaleb, "Hierarchical Dental X-Ray Radiographs Matching," 2006 International Conference on Image Processing, Atlanta, GA, USA, 2006, pp. 2677-2680, doi: 10.1109/ICIP.2006.313061.

[12] K. Qing and R. Zhang, "An Efficient ConvNet for Text-based CAPTCHA Recognition," 2022 International Symposium on Intelligent Signal Processing and Communication Systems (ISPACS), Penang, Malaysia, 2022, pp. 1-4, doi: 10.1109/ISPACS57703.2022.10082852.

[13] J. Si, S. L. Harris and E. Yfantis, "A Dynamic ReLU on Neural Network," 2018 IEEE 13th Dallas Circuits and Systems Conference (DCAS), Dallas, TX, USA, 2018, pp. 1-6, doi: 10.1109/DCAS.2018.8620116.

[14] G. Lin, A. Milan, C. Shen and I. Reid, "RefineNet: Multi-path Refinement Networks for High-Resolution Semantic Segmentation," 2017 IEEE Conference on Computer Vision and Pattern Recognition (CVPR), Honolulu, HI, USA, 2017, pp. 5168-5177, doi: 10.1109/CVPR.2017.549.

[15] R. V. Kumar Reddy, B. Srinivasa Rao and K. P. Raju, "Handwritten Hindi Digits Recognition Using Convolutional Neural Network with RMSprop Optimization," 2018 Second International Conference on Intelligent Computing and Control Systems (ICICCS), Madurai, India, 2018, pp. 45-51, doi: 10.1109/ICCONS.2018.8662969